

Martin Prachař, martin.prachar@fsv.cvut.cz

WG1 - Carlos Couto, ccouto@ua.pt

WG3 - Nuno Lopes, nuno.lopes@ua.pt

WG3 - Michal Jandera, michal.jandera@fsv.cvut.cz

WG3 - Paulo Vila Real, pvreal@ua.pt

WG2 - František Wald, wald@fsv.cvut.cz

6 BENCHMARK STUDY OF LATERAL TORSIONAL-BUCKLING OF CLASS 4 STEEL PLATE GIRDERS UNDER FIRE CONDITIONS: NUMERICAL COMPARISON

Summary

This paper presents a benchmark study of the lateral torsional-buckling of class 4 steel plate girders under fire conditions, which is based on the RFCS project FIDESC4 - Fire Design of Steel Members with Welded or Hot-rolled Class 4 Cross-sections. In the framework of project FIDESC4, a number of experimental tests were carried out in the Czech Technical University in Prague to study the LTB of Class 4 beams in case of fire. The focus of this benchmark study is comparison between the numerical results obtained with the programs ABAQUS and SAFIR. The simple examples were numerically modelled by means of GMNIA (geometrically and materially non-linear analysis with imperfections) applying different finite element method (FEM) software. The geometrical imperfections combination has been used according to the Annex C of EN 1993-1-5. Detailed information on the geometric data, geometrical imperfections and actual mechanical properties are given so that other researchers can reproduce the presented case studies.

6.1 INTRODUCTION

This paper deals with lateral-torsional buckling (LTB) of slender steel I beams under fire conditions. The fire behaviour of three beams is analysed by means of numerical analysis.

Steel members with thin-walled cross-sections are commonly used in buildings due to its lightness and long span capacity, and the understanding of the fire resistance of these structural elements can still be further developed and increased.

The structural steel elements with thin walled cross-sections (Class 4 section according to Eurocode 3 (CEN, 2005)) subjected to uniform bending diagram, are characterized by having the possibility of occurrence of failure by both local and global lateral-torsional buckling modes (LTB). These instability phenomena and their influence on the ultimate strength are of upmost importance to

characterize the behaviour of these members. The local buckling occurs due to the compression of thin plates in profiles cross-sections (see Fig. 6.1a). The LTB is an instability phenomenon that in I-sections is induced by the compressed flange of unrestrained beams subjected to bending around the major axis as shown in Fig. 6.1b.

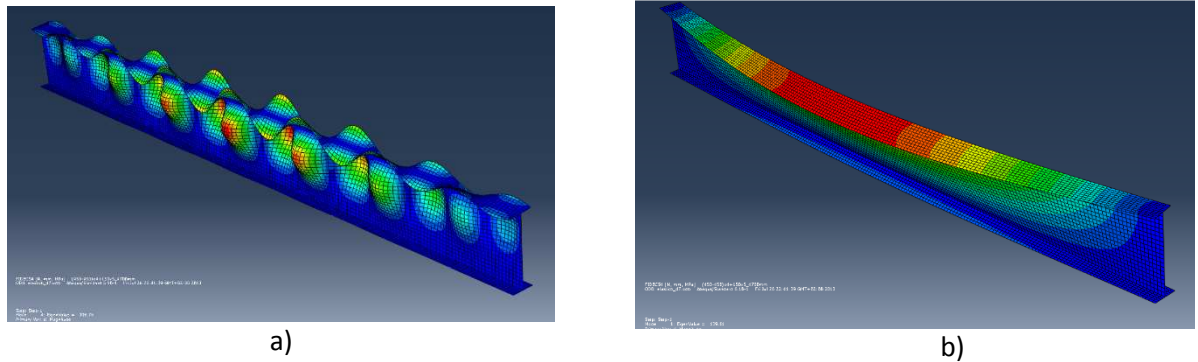


Fig. 6.1 Buckling mode shapes: a) local buckling b) lateral-torsional buckling

Three of the investigated numerical models are presented. Two packages of FEM software were used, the commercial software ABAQUS and the specially developed programme for fire structural analysis SAFIR (Franssen, 2005). The results of the FE analyses are compared between them, and the used input is specified as benchmark tests proposal for future researchers willing to validate new software, new simulations techniques or analytical solutions.

6.2 CASE STUDY (DESCRIPTION OF THE BENCHMARK STUDY)

A simply supported beam with two equal concentrated loads applied symmetrically was modelled (see Fig. 6.2). The central part of the beam of 2.8m (between the point loads), which was therefore subjected to uniform bending, was the only heated part. The simulation set-up is shown in Fig. 6.2b. The two load applications points were laterally restrained and point pinned supports were applied at the beams end extremities.

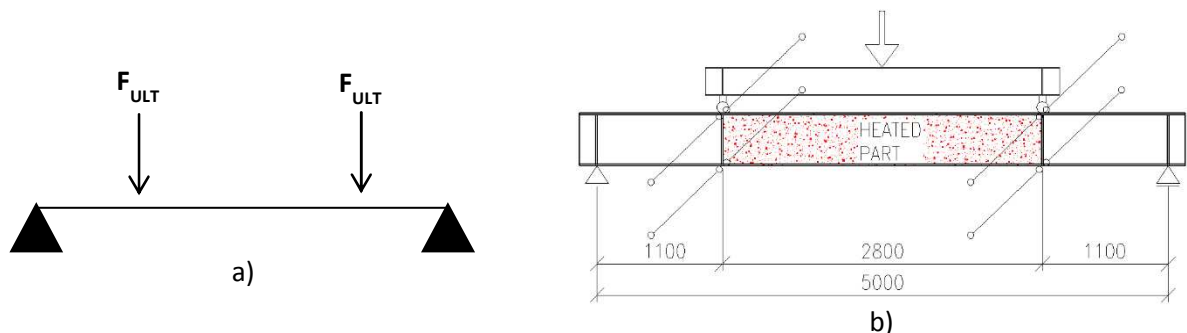


Fig. 6.2 Tested beam: a) scheme; b) test set-up

The three simulations differ in the cross-sections and applied temperatures were made. Tab. 6.1 presents the used cross-sections. Two simulations were performed on beam with constant cross-section. One simulation was performed on a tapered beam (height of the web varies linearly from one end to another). The simulations for section 1 and 2 were set to be at 450°C and simulation for section 3 at 650°C.

The end plates (stiffeners at supports) were made of 10 mm thick plate and the web stiffeners under the load were 20 mm thick. Figure 6.3 summarises the beams dimensions.

Tab. 6.1 Cross-sections

	Heated Cross-section [mm]		Non-heated Cross-section [mm]	
	Dimensions [mm]	Idealized dimensions (FEM)	The same as in the heated part See Fig. 6.3a	
Test 1 (450°C)	$h = 460$ $b = 150$ $tf = 5$ $tw = 4$			
Test 2 (450°C)	<p>Middle span</p> $h = 460$ $b = 150$ $tf = 7$ $tw = 4$	<p><u>MIDDLE SPAN</u></p>	<p>Side span</p> $h = 460$ $b = 150$ $tf = 7$ $tw = 5$ (see Fig. 6.3b)	<p><u>SIDE SPAN</u></p>
Test 3 (650°C) (Tapered beam, see Fig. 6.3c)	$hA = 460$ $hB = 620$ $b = 150$ $tf = 5$ $tw = 4$	<p><u>SECTION A</u></p>	<p><u>SECTION B</u></p>	

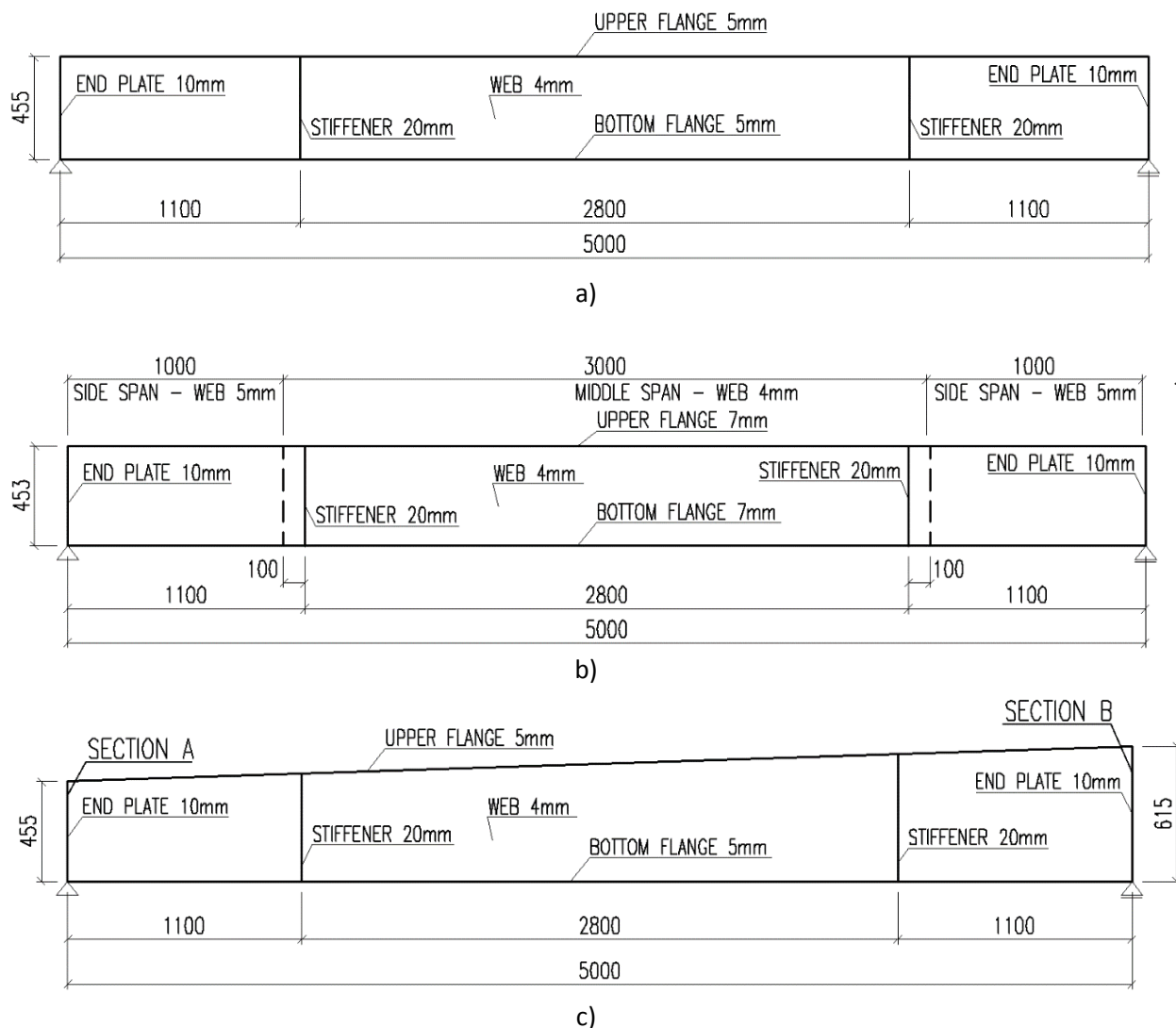


Fig. 6.3 Beams: a) test 1; b) test 2; b) test 3

6.3 NUMERICAL ANALYSES

To consider the local buckling of thin walls in members with Class 4 cross-sections, shell finite elements were used instead of the beam finite elements, due to the fact that it is one of the dominant failure modes.

As mentioned before, two finite element programs were used, ABAQUS and SAFIR. The software SAFIR (Franssen, 2005) is a geometrical and material non-linear finite element code especially developed, at the University of Liège, to model the behaviour of structures in case of fire. The ABAQUS code is a general software for finite element analysis. It allows a complete solution for a large range of problems, including the analysis of structures under fire.

6.3.1 Boundary and loading conditions

The restrictions applied to the model follow the degrees of freedom provided by the supports and the lateral restraints on Fig. 6.2 as it is presented in Fig. 6.4. The supports were considered just by one point support at the lower flange center, see Fig. 6.5. One support restrains deformations in all directions, all rotations were free. The second allowed also deformation in direction along the beam axis. The cross-section was transversally restraint in the section where load was applied.

In these numerical models, it was considered that the applied loads were controlled by forces but also by displacements.

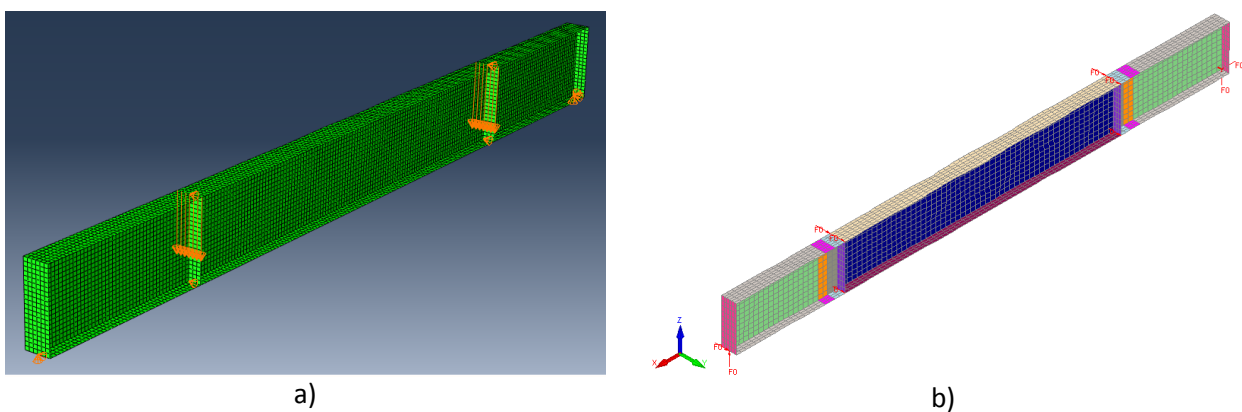


Fig.6.4 Numerical model used: a) in ABAQUS b) in SAFIR



Fig. 6.5 Pin point supports: a) free; b) fixed

6.3.2 Material properties

The beam was made of steel grade S355, see Tab. 6.2. All material properties (yield strength and young modulus), which were adopted into the models, are based on the EN 1993-1-2:2005. The thermal expansion was not considered in the analysis. The residual stresses were neglected. Elevated temperature is used for the internal span only as already described. Adjacent parts of the beam and stiffeners were considered at room temperature.

Tab. 6.2 Cross-sections

Yield stress f_y	355 MPa
Elastic modulus	210 GPa
Poisson constant	0.3

6.3.3 Initial imperfection

Initial geometric imperfections were applied following the elastic buckling eigenmodes. Two shapes were chosen: the beam 1st local buckling mode and 1st global buckling mode (LTB) shapes (Fig. 6.6). For the imperfection amplitudes, there was used 80% of the fabrication tolerance magnitude given in EN1090-2:2008+A1 (CEN, 2011) as suggested in EN1993-1-5 (CEN, 2006). The combination of imperfections according to EN1993-1-5 was taken into account, which means using the leading buckling mode with the full amplitude but the other mode (with higher critical stress) using amplitude reduced by 0.7. The initial global and local imperfections were considered using following amplitudes:

- global = $L/750 * 0.8$ (*0.7 in case the local buckling mode has lower critical stress)
 where L is the distance between lateral supports
- local = $H/100 * 0.8$ (*0.7 in case the global buckling mode has lower critical stress)
 where H is the web height

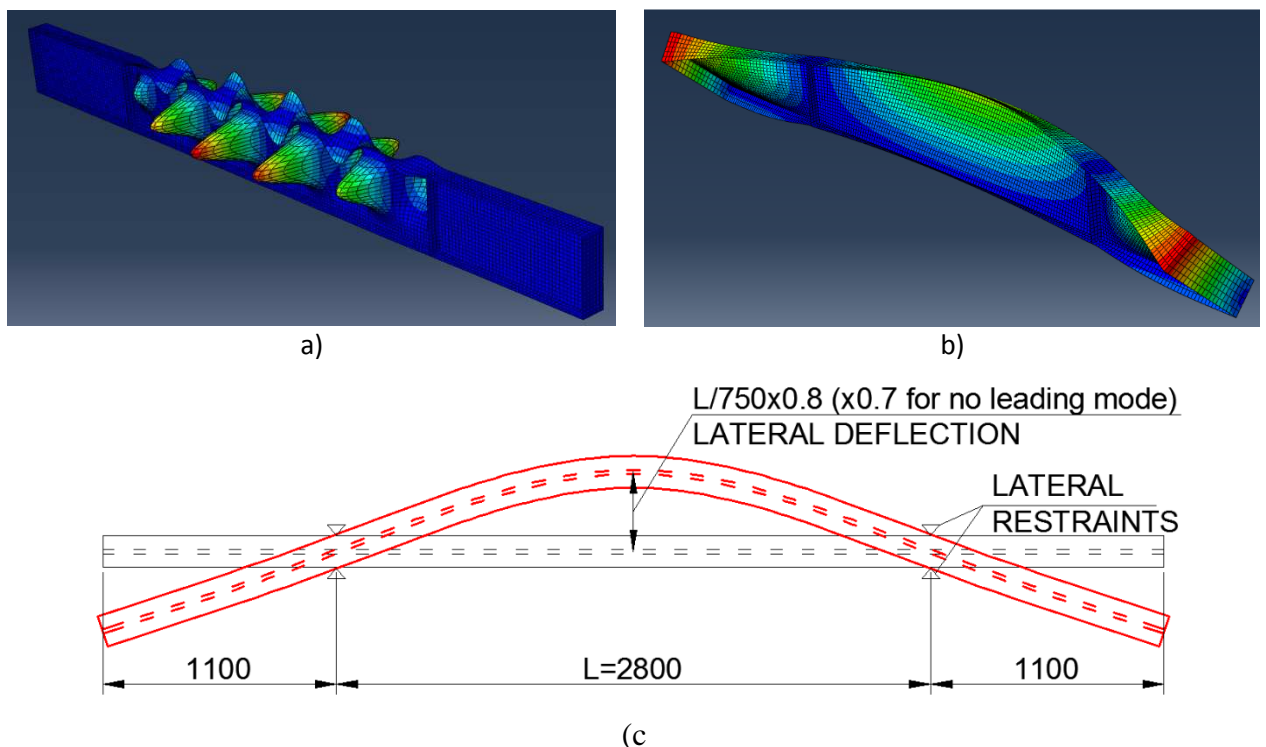


Fig. 6.6 Beams buckling modes shape: a) local; b) global; c) global - amplitude

6.3.4 Description of Abaqus model

The beam was meshed using quadrilateral conventional shell elements (namely type S4). Conventional shell elements discretize a body by defining the geometry at a reference surface. In this case the thickness is defined through the section property definition. Conventional shell elements have displacement and rotational degrees of freedom. Static calculation is used only.

Element type S4 is a fully integrated, general-purpose, finite-membrane-strain shell element. The element has four integration points per element, see Fig. 6.7

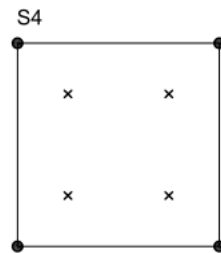


Fig. 6.7 Shell element S4 (points indicates nodes, cross indicates integration points)

The material law was defined by elastic-plastic nonlinear stress-strain diagram, where enough data points were used for it.

For definition of mesh size in ABAQUS model, there were used 6 elements for flange width and 20 elements for web height. Along the beam, there were used 4 elements per 100 mm, see Fig. 6.8

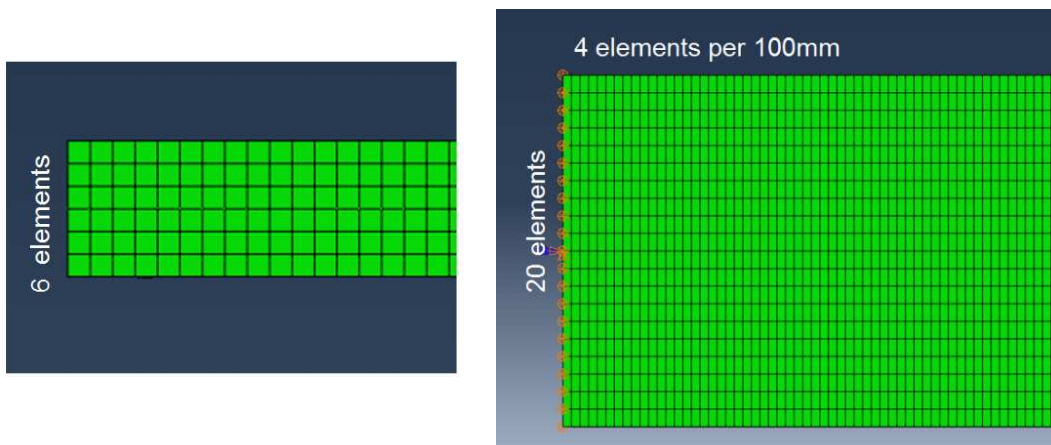


Fig. 6.8 Numbers of element on beam

6.3.5 Description of Safir model

In SAFIR, the beams were discretized into several quadrangular shell elements with four nodes and six degrees of freedom (3 translations and 3 rotations), see Fig. 6.9 These shell elements adopt the Kirchoff's theory formulation with a total co-rotational description and have been previously validated.

The steel material law, contemplated in the software, is a two-dimensional constitutive relation according to the non-linear stress-strain formulae, according to part 1-2 of the EC3 and the von Mises yield surface. Dynamic calculations were performed, and the mesh used is indicated in Fig. 6.10.

The program SAFIR possesses two distinct calculation modules: one for the thermal behaviour analysis; and another one for the mechanical behaviour analysis of the structure. The non-uniform temperature evolution is calculated for each existing section type in the structure (thermal analysis). Subsequently, the mechanical module of the program reads these temperatures and determines the thermo-mechanical behaviour of the structure in an incremental analysis (structural analysis).

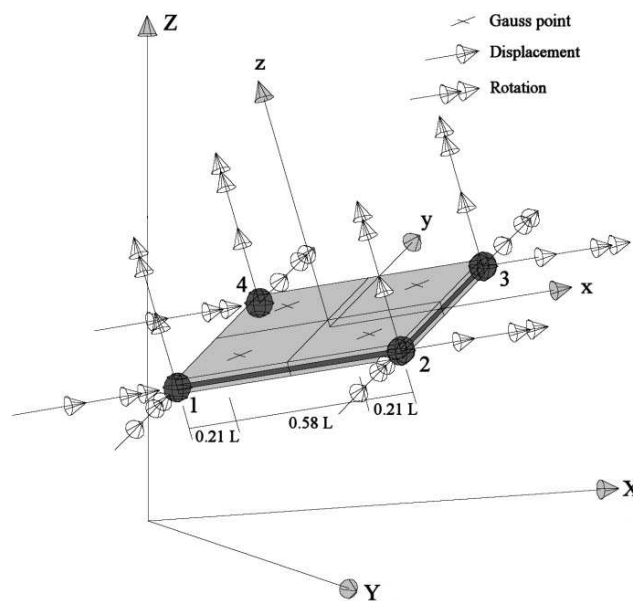


Fig. 6.9 Shell element in SAFIR

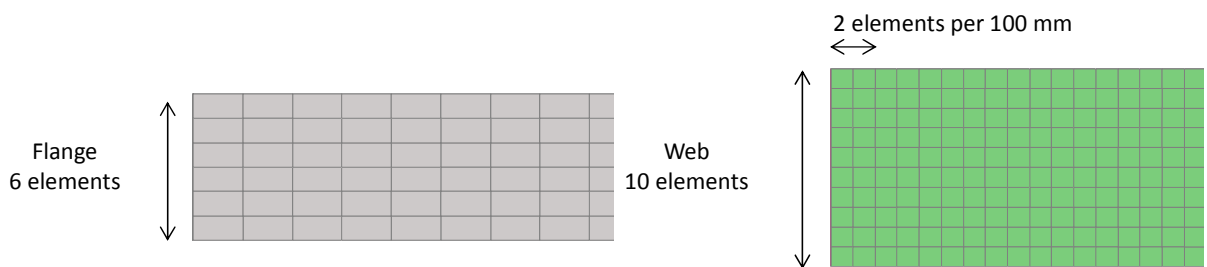


Fig. 6.10 Numbers of element used in the mesh

6.4 DISCUSSION OF THE RESULTS

Fig. 6.11 shows the failure deformed shape of the beam with cross-section no. 1 obtained from the numerical analyses.

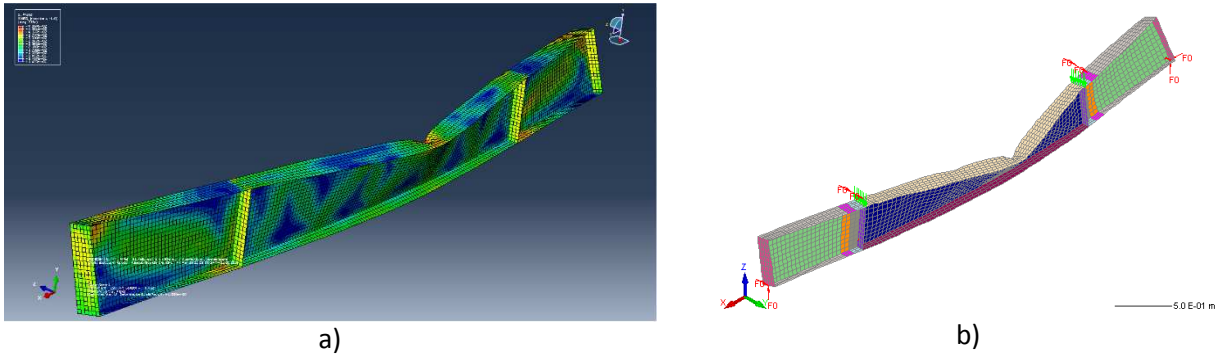


Fig. 6.11 Failure deformed shape on the: a) Abaqus analysis; b) Safir analysis

The numerical models results are analysed in Fig. 6.12 and Tab. 6.3. This figure shows the load-displacements relationship comparisons between the numerical analyses. The load corresponds to the total force imposed on the two load application points. The shown displacement corresponds to the vertical displacement at the bottom flange at mid span. In the charts the curves corresponds to the results of the models.

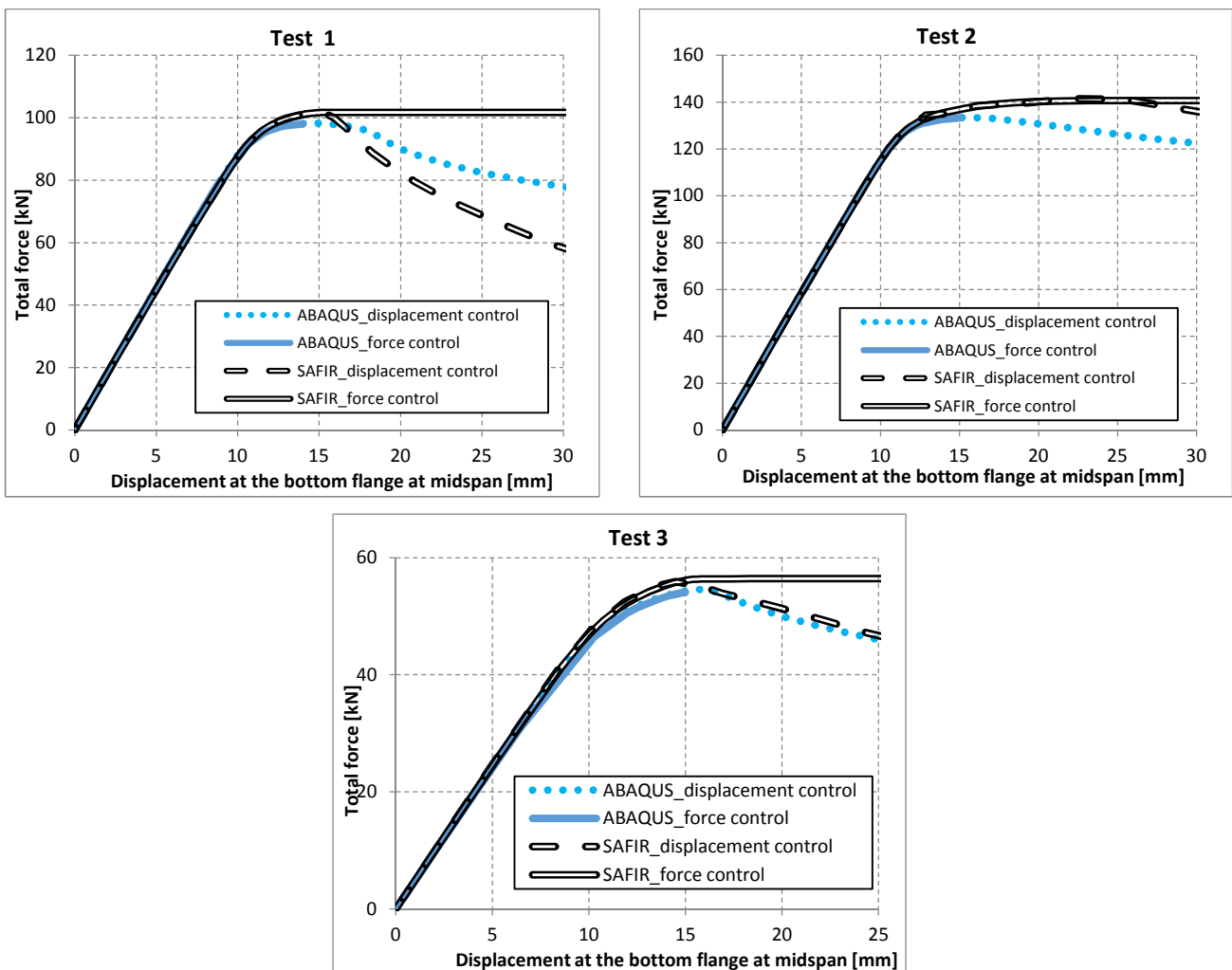


Fig. 6.12 Load-displacement relation for the three beams

From the charts it can be concluded that the two programs give results and mechanical behaviours at high temperatures that are close from each other. Recapitulation of results is shown in Tab. 6.3

Tab. 6.3 Comparison between Numerical models

Comparison between Numerical models (ABAQUS vs. SAFIR)				
Test number	Loading conditions	Total force [kN]		Ratio
		ABAQUS	SAFIR	(SAFIR/ABAQUS)
TEST 1	Displacement control	98.21	101.54	1.034
	Force control	98.01	101.67	1.038
TEST 2	Displacement control	133.43	141.39	1.060
	Force control	133.20	140.73	1.057
TEST 3	Displacement control	54.56	55.89	1.024
	Force control	54.33	56.46	1.039

6.5 BENCHMARK STUDY PROPOSAL

The above described cases studied can be used as benchmark studies. For future researches on the topic, all needed input data are given in this paper and summarised on Tab. 6.4.

Tab. 6.4 Input data

Dimensions	
Cross-section dimensions	(Tab. 6.1)
Beams total length (for all beam)	5000 mm (Fig. 6.2b)
Heated beam length, length between lateral restraints and concentrated loads (for all beam)	2800 mm (Fig. 6.2b)
End plates thickness (for all beam)	10 mm
Stiffeners thickness at the load application points (for all beam)	20 mm

Boundary and loaded conditions	
Lateral restraints on the upper and bottom flanges at load applications points	Fig. 6.2b and 6.4
Supports	Fig. 6.2b and 6.5
First the beam is heated and only after the forces are applied	steady state
Loads application (controlled by)	Displacements/ Force

Material properties	
Steel plates yield strength	Tab. 6.2
Steel plates young modulus	Tab. 6.2
Reduction of material properties	Paragraph 6.3.2
Steel temperatures	Tab. 6.1
Residual stresses	NO
Thermal expansion	NO

Imperfections	
Geometric imperfections shapes	1 st local plus 1 st global buckling modes
Leading mode Test 1	Global buckling mode
Leading mode Test 2	Global buckling mode
Leading mode Test 3	Global buckling mode
Geometric imperfections maximum amplitudes	6.3.3

Several output data can be analysed. The first suggestion corresponds to the comparison presented on the previous section, regarding the relationship between the applied load (2xF) and the vertical displacement at the bottom flange at mid span. However, other displacements and rotations such as lateral displacements on the upper flanges or rotation at the supports or even stresses distribution are also important to better understand the behaviour of the beams.

6.6 SUMMARY

This paper presents numerical modelling using two different FEM software packages, on three fire resistance tests to steel beams with slender I-cross-sections. The results are reasonably close between them and it can be concluded that the mechanical behaviour during the complete duration of the fire tests to the beams was fairly predicted by the numerical tests. All needed data for future simulations, experimental tests or analytical validations was described.

Acknowledgement

The authors would like to thanks the financial support by the European Commission through the Research Fund for Coal and Steel for research project FIDESC4 “Fire Design of Steel Members with Welded or Hot-rolled Class 4 Cross-section”.

References

- ABAQUS: Analysis user's manual, Volumes I-IV, version 6.10. (2010). Hibbitt, Karlsson & Sorenses, Inc., Providence, R.I, USA.
- Franssen JM, "SAFIR A Thermal/Structural Program Modelling Structures under Fire", *Engineering Journal* vol 42/3, 143-158, 2005.
- CEN European Committee for Standardisation, EN 1993-1-1, Eurocode 3, Design of Steel Structures - Part 1-1: General rules and rules for buildings, Brussels, Belgium, 2005.
- CEN European Committee for Standardisation, EN 1993-1-5, Eurocode 3: Design of Steel Structures - Part 1-5: Plated structural elements, Brussels, Belgium, 2006.
- CEN European Committee for Standardisation, EN 1090-2:2008+A1, Eurocode 3: Execution of steel structures and aluminium structures - part 2: Technical requirements for steel structures, Brussels, Belgium, 2011.